International Research Journal of Engineering and Technology (IRJET) e-ISSN: 2395-0056
Volume: 03 Issue: 01 | Jan-2016 www.irjet.net p-ISSN: 2395-0072

# Numerical and Experimental investigation of packed bed thermal energy storage system with $Al_2O_3$ Nanofluid

**G.SrinivasRao, P. Vemkateswa Rao**

*Department of Mechanical Engineering*
*Kakatiya Institute of Technology & Science*
*Warangal, Telangana, INDIA*

## Abstract

*This paper presents the results of a numerical investigation on the transient behaviour of a packed bed thermal storage unit using Al203 nanofluids. The storage material consists of tightly spherical particles of glass beads and pebbles, packed in a reservoir wherein the heat transport fluid flows from the bottom to the top in the charging phase only. The process of charge of the storage system gives rise to a typical temperature distribution along the flow direction defined "thermocline". The main objective of this work is to analyze the temperature distribution along the storage system and the estimation of enhancement ratio and advantage ratio of storage system with nanofluid in comparison with water. The numerical investigation is based on a two-phase one-dimensional modified Schumann model, where thermodynamic properties of the fluid are temperature dependent*

***Keywords:*** *Packed Bed, Thermal Energy Storage, Advantage Ratio, Enhancement Ratio, Nanofluid*

## 1. INTRODUCTION

Thermal power plants based on solar energy are considered one of the most promising technologies to reduce the impact of greenhouse gases produced by conventional power generation systems. In particular, CSP (Concentrating Solar Power) plants have the greatest potential of development, because by increasing the plant size the cost of energy storage (TES) system to allow solar power plants to operate with continuity and independently from sunshine intensity and availability. In this way, the storage system becomes a strategic component of a solar power plant, ensuring great flexibility. Moreover, TES used in several industrial and commercial applications are nowadays often integrated with different sources of heat. Different storage methods convert solar radiation into thermal energy that can be stored as sensible heat, latent heat or chemical energy [3-7]. Storage of sensible heat is achieved by increasing storage medium temperature, latent heat energy is stored using phase change materials (PCM) whilst thermo-chemical storage involves reversible chemical reactions. Latent heat and chemical energy are considered the most promising technologies. However, sensible heat storage is the simplest and cheapest method to store thermal energy and some technological and economical aspects make it superior; it is still the most suitable storage technique used in air-based solar system [8] TES can be classified as active or passive systems. The former can be of the direct or indirect type [9-11]. In the case of the direct type, the storage medium is the same heat transfer fluid (HTF), whereas in the indirect method a second fluid is used for storing the heat. In passive storage systems a solid material is used as storage medium and the HTF passes through the storage medium only during the charging and discharging phases [12]. When the heat transfer fluid is a liquid such as oil or molten salt, there are technical and operational problems in addition to the high costs. For example, molten salts have a relatively high freezing temperature (120-220°C) which entails high costs of maintenance and operation. Oils are flammable and corrosive and due to their thermal stability the working temperature is kept up to 400°C with the freezing point at about 10°C. To reduce costs of the storage system, in recent years TES systems with a single tank filled with solid material of high thermal capacity have been proposed. A storage system with a single tank thermocline is about 35% cheaper than a system with two storage tanks [13]. In the system with a single tank, the hot and cold fluids are separated by stratification within a packed bed of solid material and the region between the coldest fluid and the hottest one, called thermocline, is characterized by a strong gradient of temperature that mainly depends on the characteristics of the storage material. Among solid materials, the most promising are refractory ceramic materials, concrete, limestone, steatite et sim., for their relatively low cost and high thermal capacity. In these systems, the most important requirements are the energy density of the storage material (storage capacity), the heat transfer coefficient and compatibility (safety) between the HTF and the solid material, the mechanical and chemical stability of the storage material, the reversibility for repeated charging and discharging cycles (lifetime), the thermal energy loss and the stratification of the fluid [14]. Systems with packed bed solid material have been widely

studied, and many published works on fixed bed energy storage use the model originally developed by Schumann [8, 15-19]. In this work a numerical investigation on the transient behaviour of a packed bed thermal storage unit was carried out considering alumina balls of small diameter as storage material and air, diathermic oil and molten salt as HTF fluid. The main objective of this work is to analyze the behaviour of the storage system, focusing on the phenomenon of hysteresis that occurs for repeated cycles of charge and discharge, and verify the influence of different operating parameters on performance and charge capacity. This aspect is rarely studied in literature [20, 21], but it is important to determine the effective storage capacity of the reservoir which inevitably affects performance. Finally, the paper describes the behaviour of the storage system when fed according to the typical radiation of a summer day, which involves a variable input thermal power. The molten salt mixture can be used between 260°C and 600°C, the mixture begins to crystallize at 238°C and is completely solid at 221°C [23]. The range between 150- 550°C matches well with commercial steam power plants often used nowadays in CSP systems [2, 24]. This range of temperature can be achieved with air which, compared to the other two fluids, has a lower heat capacity and density and a higher pressure loss because of its high velocity during the thermal process. The three fluids work at different pressures: air and molten salts can be used at atmospheric pressure while diathermic oils at high temperature need to be pressurized (vapour pressure >1 MPa at 400°C).

As in many published works on TES systems with a fixed bed, this model is also based on the work originally developed by Schumann [17]. It is a two phase-one dimensional model which enables calculation of the time evolution of the spatial distribution of both solid and fluid temperature. The temperature of both phases is evaluated along the flow direction within the points chosen for the spatial discretization, according to existence literature.

The model assumes uniform characteristics in the radial direction [25], while the physical properties of the solid material are kept constant; the HTF properties are function of pressure and temperature. The Biot number of the particles is small enough to assume as uniform the temperature distribution inside the sphere. The main heat transfer mechanism considered is forced convection, whilst radiation is neglected for both phases and thermal conduction is considered only for the fluid because spherical particles have a very small contact surface. The pressure drop, along the bed is evaluated with the Ergun equation [26, 27]. Due to the thick layer of insulating material, the thermal losses are neglected. Here the volumetric convective heat transfer coefficient hv between the solid particle and fluid is linked to the convective heat transfer coefficient α: As reported in [21], the heat transfer coefficient α can be calculated for air according to the Coutier and Faber correlation [15] as a function of mass flow rate per unit cross section G and particle diameter: For oil and molten salts the Wakao and Kaguei correlation is used [28], as reported in ref. [25] for oil and in ref. [29] for molten salts: The influence of these parameters for different charging phases using a gaseous fluid was discussed in depth in [30].

The main objective of this study is to analyze the thermal behaviour of a sensible heat storage system characterized by a solid storage material of high volumetric thermal capacity. The solid material consists of spherical particles tightly poured into a vertical reservoir, wherein the HTF flows from the bottom to the top of the tank during the charging phase. Water and Al2o3 with three different concentrations are the HTF considered in this work and spherical particles of two different sizes glass beds are the solid material.

**Table 1. Working process parameters**

| | |
|---|---|
| Maximum temperature [°C] | 55 |
| Minimum temperature [°C] | 40 |
| Aspect Ratio Lb/D | 12.5 |
| Length of bed[mm] | 500 |
| Bed void fraction | 0.39 and 0.49 |
| Particle diameter [mm] | 6, 14.56 |
| Nanofluid concentration [%] | 0.02, 0.1,0.5 |
| Mass flow rate [LPH] | 150,200,250,300 |

Table 1 reports the range of temperature operation of the bed with three water and three different concentration Al203 nanofluids. This range of temperature can be achieved with water which, compared to the nanofluid fluid. The two fluids work at same operating input conditions. The performance of the storage system is evaluated considering two important parameter one is advantage ratio and other is enchantment ratio shown in equations (1) and (2)

Based on the experimental results two terms are considered. They are Advantage ratio and Enhancement ratio and defined as follows

$$\text{Advantage ratio} = \frac{\text{Heat Transfer}}{\text{Pressure drop X Discharge in m}^3/\text{sec}} \quad (1)$$

$$\text{Enchancement ratio} = \frac{\frac{HTC_{nf} - HTC_{bf}}{HTC_{bf}}}{\frac{Pressure drop_{nf} - Pressure drop_{bf}}{Pressure drop_{bf}}} \quad (2)$$

**2.0 MATHEMATICAL MODEL :** The traditional Schumann [1929] model extended by Hughes et al. [1976] and later by Sagara & Nakahara [1991] formed the analytical framework for estimating the thermal behavior

of packed beds at high flow velocities.

The energy balance for the fluid can be written as:

Energy supplied by the fluid = Energy transferred to bed by convection + Energy leaving the bed with flowing fluid + Energy loss to the atmosphere.

Assuming the heat energy to the atmosphere to be negligible, the energy balance equation can be written as

$$m_f C_{pf} T_{fi} = h_v A\left(T_f - T_b\right) dz + m_f C_{pf}\left(T_{fi} + \frac{\partial T_{fi}}{\partial x} dz\right) \quad (3)$$

$$\frac{\partial T_{fi}}{\partial\left(z/L_b\right)} = -\frac{h_V A L_b}{m_f C_{pf}}\left(T_f - T_b\right) \quad (4)$$

Rewriting equation (4) one can obtain

$$\frac{\partial T_{fi}}{\partial\left(z/L_b\right)} = -NTU\left(T_f - T_b\right) \quad (5)$$

The equation (5.3) can be integrated to obtain the following expression

$$\int_m^{m+1} \frac{\partial T_f}{T_f - T_b} = -NTU \int \partial\left(\frac{z}{L_b}\right)$$

or

$$In\,\frac{T_{f,m+1} - T_{b,m}}{T_{f,m} - T_{b.m}} = -NTU\left(\frac{\Delta z}{L_b}\right)$$

or

$$\frac{T_{f,m+1} - T_{b,m}}{T_{f,m} - T_{b.m}} = e^{-NTU \times N}$$

or

$$\frac{T_{f,m} - T_{b,m+1}}{T_{f,m} - T_{b.m}} = 1 - e^{-NTU \times N} \quad (6)$$

where $NTU = \frac{h_V A L_b}{\dot{m}_f C_{pf}}$ and $N = \frac{\Delta z}{L_b}$

The Eq. (6) is considered to estimate the non-dimensional temperature for fluid, solved with the initial conditions given

$$Z = 0;\quad \theta_f = 1 \quad (7)$$

For the solid phase, the equation is obtained as

$$(1-\varepsilon)\frac{\partial T_b}{\partial t} = -\frac{h_V}{C_{pb}\rho_b}\left(T_f - T_b\right) \quad (8)$$

The equation (8) is transformed to obtain as

$$\frac{\partial T_b}{\partial t} = \frac{h_V}{\rho_b C_{pb}(1-\varepsilon)}\left(T_f - T_b\right) = \frac{NTU}{\tau}\left(T_f - T_b\right)$$

or

$$\frac{\partial T_b}{\partial t} = \frac{NTU}{\tau}\left(T_f - T_b\right) \quad (9)$$

where $\tau = \frac{m_s C_{ps}}{m_f C_{pf}}$

The Eq. (9) is considered to determine the temperature variation of the solid subjected to initial condition, $Z = 0, T_b = T_{bi}$

## 3.THEORITICAL AND EXPERIMENTAL DETERMINATIONS

### 3.1 FRICTION FACTOR

The pressure drop of the experiments is predicted in terms of friction factor. The experimental pressure drop is calculated by manometer, using the equation

$$\frac{P1}{\rho g} - \frac{P2}{\rho g} = \Delta h = h1 - h2$$

$$\Delta P_{\exp} = P1 - P2 = \Delta h \rho g \quad (10)$$

The experimental friction factor of water for flow in a tube is compared with Darcy equation given by

$$f = \frac{1}{2}\frac{\Delta P}{L}\frac{D_i}{\rho U_0^2} \quad (11)$$

Ergun [1956] developed the equation to calculate the pressure drop in many practical situations which is now used as a reference for all packed beds studies; the same equation is used for pressure drop presented in Eq. (12).

$$\frac{P_{in} - P_{out}}{L_b} = \frac{\mu.150(1-\varepsilon)^2 U_0}{D_p^2 \varepsilon^3} + \frac{1.75\rho(1-\varepsilon)}{D_p \varepsilon^3} U_0^{\,2} \quad (12)$$

For irregularly shaped particles, Ergun [1956] also proposed the equation for pressure drop including sphericity as reported in Eq. (12)

$$\frac{P_{in} - P_{out}}{L_b} = \frac{\mu.150(1-\varepsilon)^2 U_0}{\psi^2 D_p^2 \varepsilon^3} + \frac{1.75\rho(1-\varepsilon)}{\psi D_p \varepsilon^3} U_0^{\,2}$$

The friction factor for packed bed is calculated using the Eq.(13)

$$f = \frac{\Delta P}{L_B}\frac{D_P}{\rho U_0^2}\left(\frac{\varepsilon^3}{1-\varepsilon}\right) \quad (13)$$

### *3.2 Heat Transfer in Forced Convection*

Gnielinski [1980] developed a correlation for the estimation of Nusselt number of packed beds for single phase laminar flow of liquids under forced convection as valid for 10<Re<10,000

$$Nu = 0.664 \Pr^{0.666}\left(\frac{\mathrm{Re}}{\varepsilon}\right)^{0.5} \quad (14)$$

The Nusselt number estimated with glass beads from experiments have been compared with the values from Eq. (14).In a similar manner, Wanko [1979) presented equation [15] for forced convection through pebble beds given by

$$Nu_w = 2 + 1.1 \mathrm{Re}_p^{0.66} \Pr^{0.66} \quad (15)$$

Valid in the range of 15 < $Re_p$ < 8500.

Jeschar [1971] suggested a correlation for the estimation of convective heat transfer coefficient with pebbles in the Reynolds number range of 250 to 5500 given by

$$Nu = \frac{hD_p}{k_f} = 2.0 + \left[\frac{1-\varepsilon}{\varepsilon^2}\mathrm{Re}\right]^{0.5} + 0.005\frac{\mathrm{Re}}{\varepsilon} \quad (16)$$

250<Re<5500

**5 NUMERICAL ANALYSIS**

While calculating the Nusselt number, the hydraulic diameter of the experimental test rig is considered. Numerical and experimental values are plotted using Origin 6.0. The experimental Nusselt numbers for glass beads and pebbles are calculated and compared with forced convection with Eqs. (14) to (16).

**6 RESULTS AND DISCUSSIONS**

The numerical results are compared with the experimental data for temperature variation friction factor and Nusselt number for the working fluid is presented in the form of graphs.

**6.1 *Experiments with Glass beads***

The experimental flow diagram as shown in Figure (1). The experimental friction factor for flow of water and nanofluid in a tube packed with glass beads of 6 and 14.6mm diameter is shown in Figure 1. The friction factor for flow through the glass beads is greater than in a tube which can be observed when compared with Hazen-Poiseuille equation for plain tube. The experimental friction factor for water is in good agreement with Eq. (12) of Ergun [1956] ensuring the reliability of the experimental setup. The friction factor with glass beads of 6mm gives higher pressure drop compared to 14.6mm and increases with nanofluid concentration.

The influence of inlet temperature, particle size and nanofluid concentration on heat transfer coefficient for 300LPH flow rate is shown in Fig 3. The heat transfer coefficient increases with decrease in particle size and increases with inlet temperature. The experimental data coincides with the correlation of Gnielinski et al. [1980] given by Eq. [14] as shown in Fig 4. It can be inferred that heat transfer coefficient increases with particle Reynolds number, nanofluid concentration and inversely proportional to the size of particle.

***6.2 Experiments with pebbles***

Experimental data of friction factor for two sizes of pebbles is shown in Fig(2) for flow of water and nanofluid at different concentrations. The agreement of data with the Eq. (13) of Ergun [1957] is satisfactory.

The variation of heat transfer coefficient with particle Reynolds number is shown in Figure (4) for inlet temperatures of $55^0$C and pebble size of 16.6mm. Figure (5) and (6) shows the variation of heat transfer coefficient for inlet temperature of $40^0$C and $55^0$C respectively for a pebble diameter of 14.6mm.The experimental data presented in figures 5.16 to is compared with equations available in literature. The heat transfer coefficients are increases with increasing the nanofluid concentration and particle Reynolds numbers and good agreements with Eq. (15) and (16) respectively.

Further a regression equation for the estimation of friction factor and Nusselt number is developed based on the experimental investigations for glass beads and pebbles represented with equations (17) through (20)

**FORCED CONVECTION**

**GLASS BEADS**

For forced convection pressure drop, friction factor and Nusselt number with spherical particles the relevant equations are,

$$f_{reg} = 20.06\,\mathrm{Re}_p^{-0.317}\left(10^{-5} + \frac{\phi}{100}\right)^{0.2919} \quad (17)$$

$$Nu = 0.178\,\mathrm{Re}_p^{0.876}\left(10^{-5} + \frac{\phi}{100}\right)^{0.5310}\,\mathrm{Pr}^{-0.44} \quad (18)$$

for $500 < \mathrm{Re}_p < 2800$ $2.81 < \frac{D_t}{D_p} < 6.83$ and $\phi < 0.5\%$

**PEBBLES**

$$f_{reg} = 7.8528\,\mathrm{Re}_p^{-0.21498}\left(10^{-5} + \frac{\phi}{100}100\right)^{0.0020409}(\psi)^{-1.6318} \quad (19)$$

$$Nu_{reg} = 3.805\,\mathrm{Re}_p^{0.55307}(\psi)^{3.38488}\left(10^{-5} + \frac{\phi}{100}\right)^{-0.0098366}\,\mathrm{Pr}^{-0.92984} \quad (20)$$

Validate for $500 < \mathrm{Re}_p < 3300$, $2.41 < \frac{D_t}{D_p} < 2.81$, $\phi < 0.5\%$, $0.56 < \psi > 0.65\%$

The experimental values of friction factor are compared with the correlated values from the Eq.(17) and Eq.(19), plotted through Fig(2) to Fig (3). For Nusselt numbers are compared with Eq. (18) and Eq.(20) and drawn respectively in Fig (4) to Fig (7) between experimental data and the values estimated with from equations for glass beads and pebbles.

Parity graphs are drawn using the predicted regression equation given in Eq. 17 through Eq.20 with Fig (8) to Fig (11). The experimental friction factor, Nusselt number are shown, where in the figures and values computed from the developed regression positively matched with the experimental results. For the laminar flow of $Al_20_3$ nanofluid, the friction factor with packed glass beads has an average deviation (AD) of 4.56% and standard deviation of (SD) 5.89% when compared with water and the friction factor for pebbles has an of 1.23% and (SD) of 4.12% when compared to spherical particles. The Nusselt numbers for beds packed with spherical particles has an AV of 5.66% and SD of 6.78% when compared with plain tube.

**7.0 CONCLUSIONS**

1. The friction factor of water and nanofluid is inversely proportional to the size of the bed particle for both glass beads and pebbles.
2. The heat transfer coefficient with nanofluid at any concentration is always greater than water at similar operating conditions.
3. The heat transfer coefficient increases with flow rate, fluid inlet temperature and concentration of the nanofluid.
4. The friction factor obtained with 6mm glass beads at particle Reynolds number of 500 and 3000 is respectively 2.5 and 5.34 times greater, when compared to flow of water in a tube.
5. The friction factor with 6mm glass beads, at particle Reynolds number of 500 and 3000 is respectively 5.5 and 15 times greater for 0.5% nanofluid concentration, compared to flow of water in a tube.
6. The enhancement in heat transfer with 6mm glass beads, at particle Reynolds number of 500 and 3000 is respectively greater by and 14.6% for 0.5% nanofluid concentration, compared to flow of nanofluid in a tube.
7. Equations for the determination of friction factor and Nusselt number for the range $500 < \mathrm{Re}_p < 1800$, $2.4 < \mathrm{Pr} < 4.5$, $0 < \phi < 0.5\%$ can be estimated with the equations

$$f_{reg} = 20.06\,\mathrm{Re}_p^{-0.317}\left(10^{-5} + \frac{\phi}{100}\right)^{0.2919}$$

$$Nu = 0.178\,\mathrm{Re}_p^{0.876}\left(10^{-5} + \frac{\phi}{100}\right)^{0.5310}\,\mathrm{Pr}^{-0.44}$$

$$500 < \mathrm{Re}_p < 2800$$

$$2.81 < \frac{D_t}{D_p} < 6.83 \text{ and } \phi < 0.5\%$$

8 The friction factor for pebbles of different sizes with different sphericity is higher than spherical glass beads and

$$f_{reg} = 7.8528\,\mathrm{Re}_p^{-0.21498}\left(10^{-5} + \frac{\phi}{100}100\right)^{0.0020409}(\psi)^{-1.6318}$$

$$Nu_{reg} = 3.805\,\mathrm{Re}_p^{0.55307}(\psi)^{3.38488}\left(10^{-5} + \frac{\phi}{100}\right)^{-0.0098366}\mathrm{Pr}^{-0.92984}$$

Validate for $500 < \mathrm{Re}_p < 3300$ $2.41 < \frac{D_t}{D_p} < 2.81$, $\phi < 0.5\%$, $0.56 < \psi > 0.65\%$

9. The enhancement ratio increases with flow rate and inlet temperatures.
10 The enhancement ratio increases with particle size, inlet fluid temperature and inversely proportional to the concentration of the nanofluid.
11. Advantage Ratio (AR) increases with the concentration and bed particle size. However AR decreases with flow rates.
12. There is no significance change in enhancement ratio and advantage ratio with temperature.

**Nomenclature**

$A$ cross sectional area of tube, $\left(\frac{\pi D^2}{4}\right)$, $m^2$

a Particle surface area per unit volume of whole packed bed, $m^{-1}$

$C_p$ specific heat, $J / KgK$

$D_t$ inner diameter of the tube, $mm$

$D_a$ Darcy number, $\frac{K}{D_t^2}$

$f$ friction coefficient,

$G$ Mass flow rate per unit cross sectional area $Kg / \sec m^2$

$h$ convective heat transfer coefficient, $W / m^2K$

$h_v$ volumetric heat transfer coefficient, $W / m^3K$

$h_{\exp}$ Experimental heat transfer coefficient $W / m^{20}K$

$ID$ inside diameter , $m$

$k$ thermal conductivity, $W / mK$

$K$ Permeability m²

$L$ length of the tube, $m$

$\dot{m}$ mass flow rate, $Kg / \sec$

$Nu$ Nusselt number based on the fluid properties, $hD_p / k_f$

$NTU$ Number of transfer units

TES Thermal energy storage

$OD$ outside diameter, $m$

Pr Prandtl Number, $\mu_f Cp_f / k_f$

$\Delta P$ Pressure drop across the tube, Pa

$Pe_h$ Axial thermal Peclet number $\frac{m_f Cp_f L_b}{k_{ae}}$

$Q$ heat flow, $W$

$Q$ volumetric flow , $m^3 / \sec$

$r$ Radius , $m$

$R^*$ Nondimensional radius

Re Reynolds number, $\frac{\rho_f V_0 D_p}{\mu_f}$

$\mathrm{Re}_p$ Particle Reynolds number, $\dfrac{\rho_f V_0 D_p}{\mu_f (1-\varepsilon)}$

$Ra_f$ Rayleigh number based on the fluid properties $\dfrac{g\beta_f D_t^3 (T_h - T_c)}{(\alpha\nu)_f}$

$Ra_w$ Darcy modified Rayleigh number, $\dfrac{g\beta_f KD_t (T_h - T_c)}{(\alpha\nu)_f}$

$T$ temperature, K

$U_0$ Superficial velocity, (m/s)

$U_i$ interfacial velocity, (m/s)

$Z$ non dimensional axial length $\left(\dfrac{z}{L_b}\right)$

$u, v,$ Velocity components in axial, radial directions

$g$ acceleration due to gravity ,$m/sec^2$

$\xi_1, \xi_2, \xi_3$ Dimensionless coefficient in Eq.(4.29),(4.30)

$V, \xi_4, \xi_5$ Dimensionless coefficient in Eq.(4.41)

$U$ Bed heat loss coefficient

$y$ Group parameter in Eq.(4.27)

$U_0$ Reference velocity /superficial velocity of fluid $m/\sec$

***Greek symbols***

$\alpha$ Thermal diffusivity, $\left(\dfrac{k}{\rho C_p}\right)$, $m^2/\sec$,

$\varepsilon$ Void fraction , %

$\theta_f$ Dimensionless fluid temperature, $\left(\dfrac{T - T_\alpha}{T_{fi} - T_\alpha}\right)$

$\theta_s$ Dimensionless fluid temperature, $\left(\dfrac{T - T_\alpha}{T_{si} - T_\alpha}\right)$

$\beta$ Thermal expansion coefficient ,$K^{-1}$

$\Omega$ non dimensional values

$\mu$ dynamic viscosity, kg/m·s

$\upsilon$ kinematic viscosity, $m^2/s$

$\rho$ density, $kg/m^3$

$\tau$ non dimensional time

$\tau$ non dimensional value in Eq(5.7)

$\phi$ volume concentration of nanoparticles, %

***Subscripts***

*bf* base fluid

*eff* effective

*exp* Experiment

*h* hydraulic

*i* inner diameter

*p* nanoparticle

*th* theoretical

*w* water

*f* fluid

*nf* Nanofluid

*i* Inlet

0 Outlet

*reg* regression

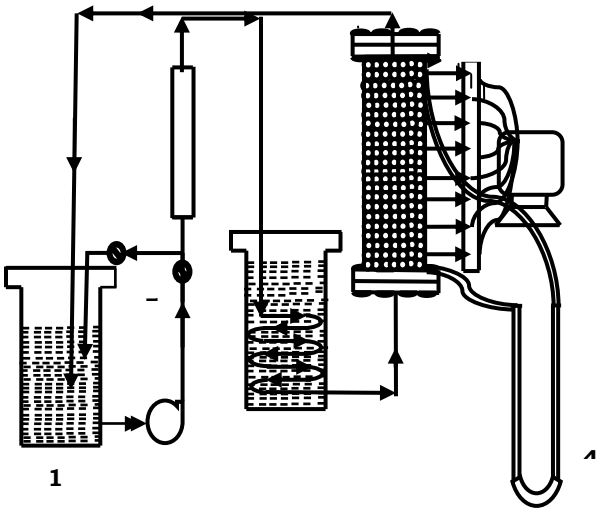


Part list: 1. Supply tank. 2. Pumping device 3. Heating tank 4. Copper coil 5.Gate valve 6. Rotameter 7.Test section 8. Data Acquisition System Tp1, Tp2 pressure taping

Fig 1 .Flow diagram for forced convection experimental setup

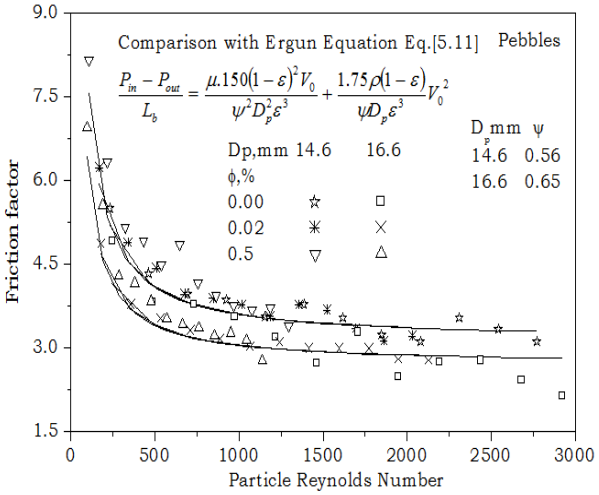

Fig2 Comparsion of theoretical and experimental friction factor in packed bed with glass beads

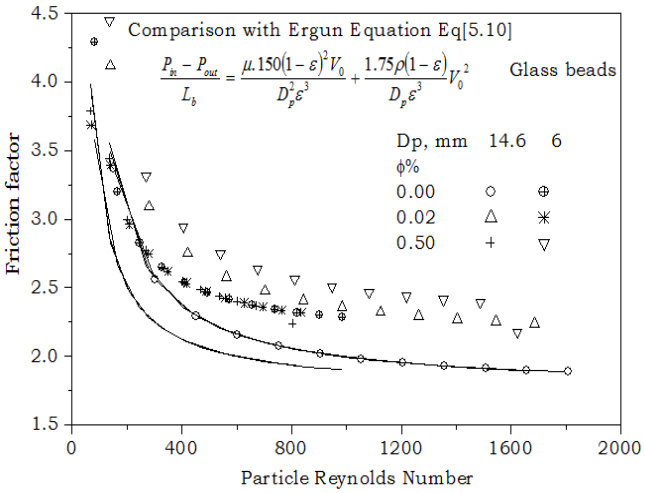


Fig3.Comparsion of theoretical and experimental friction factor with effect of particle size and sphericity for pebbles

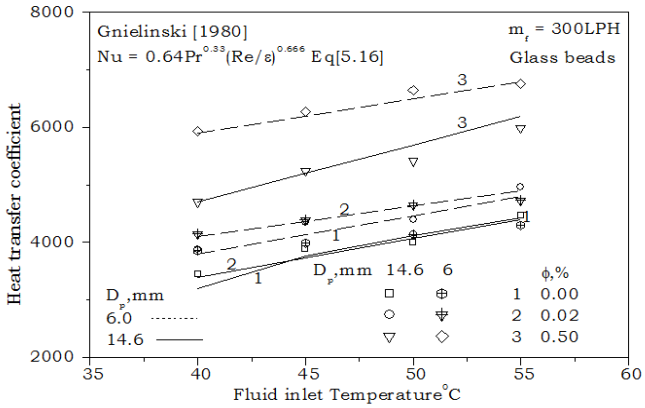


Fig 4 Effect of fluid inlet temperature, particle size and nanofluid concentration on heat transfer coefficient

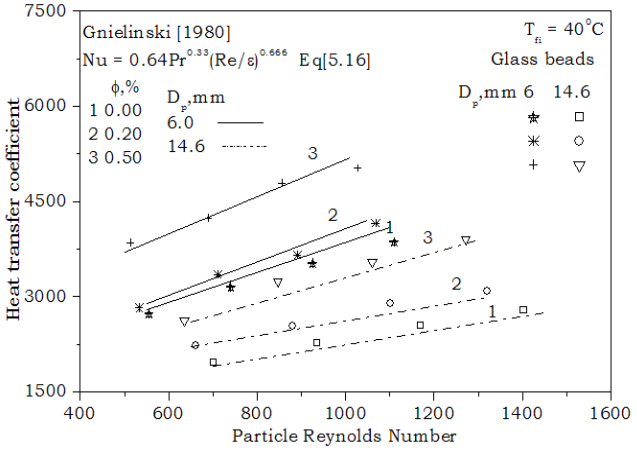


Fig5 .Effect of particle size, nano fluid concentration and flow rate on heat transfer coefficient

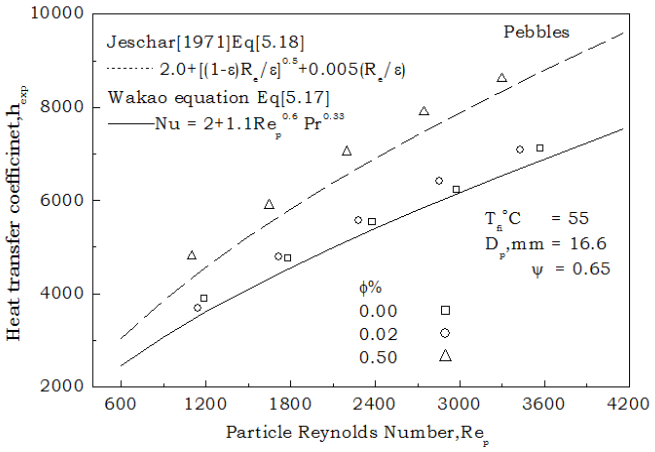


Fig 6. Effect of flow rate and concentration of nanofluid on heat transfer coefficients for pebble.

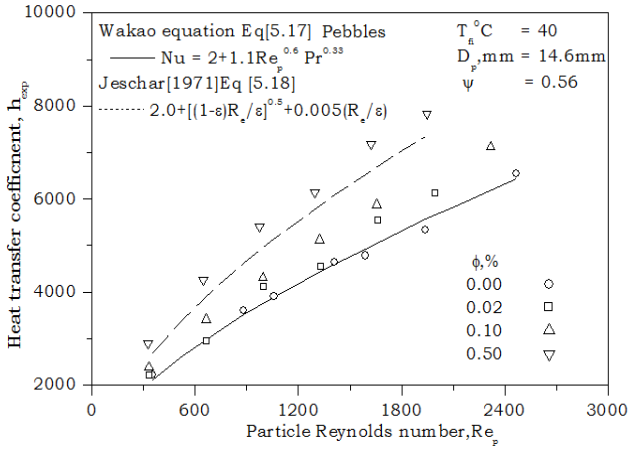


Fig 7 Effect of concentration and flow rate on heat transfer coefficients for pebbles at higher fluid inlet temperature

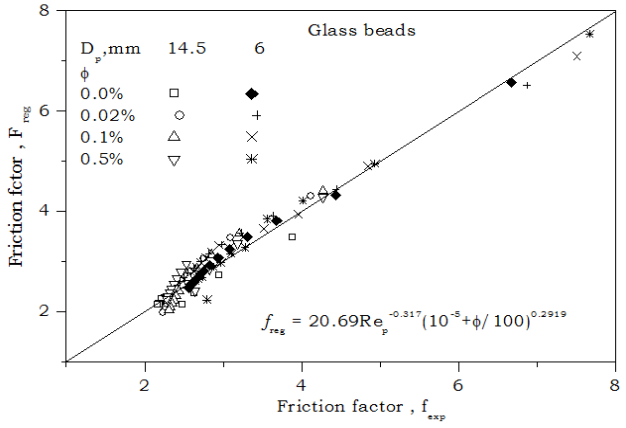

Fig 8 Comparison of calculated and experimental friction factor for glass beads

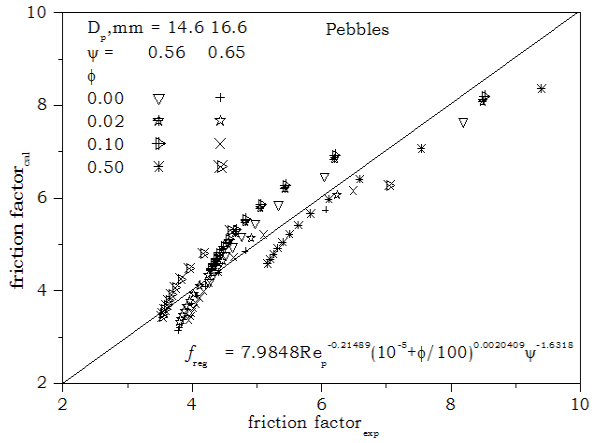


Fig 9 Comparison of experimental and calculated Nusselt number for glass beads

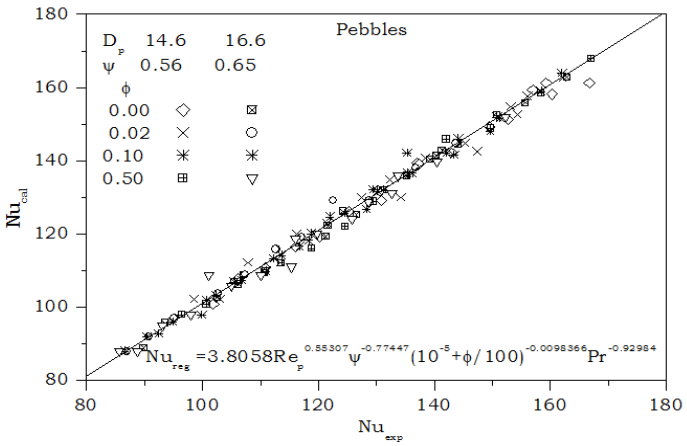


Fig 10 Comparison of calculated and experimental friction factor for pebbles

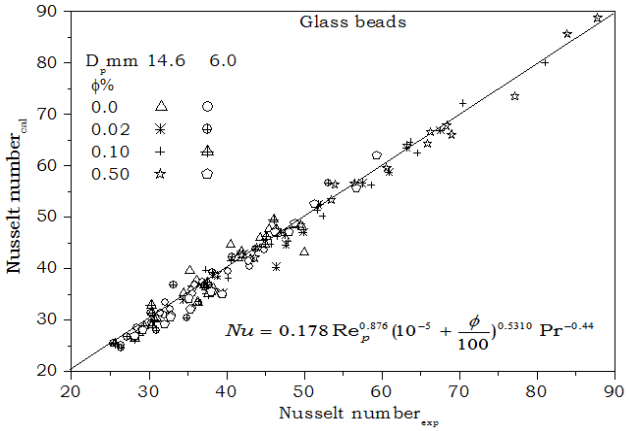


Fig11 .Comparison of calculated and experimental Nusselt numbers for Pebbles

## References

1] Concentrated-Solar Thermal-Power Plants. ESTIA Settembre 2005

[2] F. Trieb, C.Schillings, M. O'Sullivan, T. Pregger, C. Hoyer-Klick, Global Potential of Concentrating Solar Power. German Aerospace Center, Institute of Technical Thermodynamics: DLR: SolarPaces Conference Berlin, 2009.

[3] Urbani M., Corsi N., Confronto tra diversi sistemi di accumulo di energia, 6° Congresso Nazionale CIRIAF, Perugia, 2006.

[4] Dinc¸er I, Rosen MA. Thermal energy storage, systems and applications, New York: Wiley; 2002.

[5] Hasnain SM. Review on sustainable thermal energy storage technologies, part I: heat storage materials and techniques, Energy Conversion Management 1998, 39, 1127–38.

[6] Herrmann U, Geyer M, Kearney D. Overview on thermal storage systems, Workshop on Thermal storage for Trough Power Plants. FLABEG Solar International GmbH; 2006

[7] Pilkington Solar International, GmbH, Survey of thermal storage for parabolic trough power plants, National Renewable Energy Laboratory; 2000 [SR-550-27925].

[8] Antoni Gil et al., State of the art on high temperature thermal energy storage for power generation. Part 1—Concepts, materials and for power generation. Part 1-modellization, Renewable and Sustainable Energy Reviews 14 (2010)

[9] Gil A., Medrano M., Martorell I., Lazaro A., Dolado P.,Zalba B., et al. State of the art on high temperature Concepts, materials and modellization, Renewable & Sustainable Energy Reviews, 14, 31–55. 2010,

[10] Gil A., Medrano M., Martorell I., Lazaro A., Dolado P., Zalba B., et al. State of the art on high temperature for power generation. Part 2- Case studies. Renewable & Sustainable Energy Reviews, 14, 56–72. 2010,

[11] Kearney D, Kelly B, Price H. Thermal storage commercial plant design study for a two-tank indirect molten salt system, National Renewable Energy Laboratory, [NREL/SR-550-40166]. 2006

[12] Tamme R, Laing D, Steinmann WD, Zunft S. Innovative thermal energy storage technology for parabolic trough concentration solar power plants, Proceedings EuroSun 2002, the 4th ISES Europe Solar Congress, 2002.

[13] Brosseau D, Kelton JW, Ray D, Edgar M, Chisman K, Emms B. Testing of thermocline filler materials and molten-salt heat transfer fluids for thermal energy storage systems in parabolic trough power plants. J Solar Energy Eng-Trans ASME;127: 109–16 2005.

[14] D. Crandall, E. Thacher, Segmented thermal storage, Sol. Energy 77 (4)) 435e440. (2004

[15] J. Coutier, E. Farber, Two applications of a numerical approach of heat-transfer process within rock beds, Sol. Energy 29 (6) 451- 462. (1982)

[16] G. Adebiyi, E. Nsofor, W. Steele, A. Jalalzadeh-Azar, Parametric study on the operating efficiencies of a packed bed for high-temperature sensible heat storage, ASME J. Sol. Energ. Eng. 120 (12-13.) (1998)
[17] T. Schumann, Heat transfer: a liquid flowing through a porous prism, J. Franklin Inst. 208 405-416 (1929).
[18] K. Ismail, R. Stuginsky, A parametric study on possible fixed bed models for pcm and sensible heat storage, Appl. Therm. Eng. 19 (7) 757-788. (1999)
[19] Harmeet Singh, R.P. Saini, J.S. Saini, A review on packed bed solar energy storage systems, Renewable and Sustainable Energy Reviews, Volume 14, Issue 3, April Pages 1059–1069, 2010,.
[20] C. Singh, R.G. Tathgir, K. Muralidhar, Energy storage in fluid saturated porous media subjected to oscillatory flow, Heat Mass Transfer 45 (4) 427-441, (2009)
[21] M. Hänchen, S. Brückner, A. Steinfeld, High-temperature thermal storage using a packed bed of rocks-Heat transfer analysis and experimental validation, Applied Thermal Engineering 31 1798-1806,(2011)
[22] Solutia Technical Bulletin 7239115B, Therminol® VP-1, Vapor Phase/Liquid Phase Heat Transfer Fluid. 1999,
[23] Ferri R., Cammi A., Mazzei D., Molten salt mixture properties in RELAP5 code for thermodynamic solar applications. International Journal of Thermal Sciences; 47 1676–1687. (2008):
[24] R. Aringhoff et al., Concentrated Solar Thermal Power – Now! (Cecilia Baker, 2005).
[25] A. Bruch, J.F. Fourmigué and R. Couturier, "Experimental Investigation of a Thermal Oil Dual-Media Thermocline for CSP Power Plant", CEA/INES, Laboratoire des Systèmes Thermiques (LETh), BP 332, 50 avenue du Lac Léman, F-73377 Le-Bourget-du-lac, France
[26] K. Sagara, N. Nakahara, Thermal Performance and pressure drop of rock beds with large storage materials, Solar Energy, Vol. 47, n. 3, pp. 157-163, 1991.
[27] K.G.T Hollands, H.F. Sullivan, Pressure Drop across rock bed thermal storage system, Solar Energy, Vol. 33, n. 2, pp. 221-225, 1984.
[28] Wakao, N., Kaguei, S., "Heat and Mass Transfer in Packed Beds", Gordon and Beach, New York., 1982
[29] Z. Yang, S. V. Garimella "Thermal analysis of solar thermal energy storage in a molten-salt thermocline" Solar Energy 84 974–985,(2010)
[30] M. Cascetta, G. Cau, P. Puddu, "Accumulo termico ad alta temperatura per impianti solari termodinamici" 65°Congresso Nazionale ATI, Settembre 2010

SrinivasRao G. has completed his bachelor in Mechanical engineering, master in Thermal sciences and Ph.D in heat transfer. Presently he is working as Assistant Professor in Mechanical engineering department in KITS Warangal Telamgana, India. His interest field of research is heat transfer, two-phase flow solar engineering, and nanotechnology heat transfer in porous medium.

Dr. P Venkateswara Rao is a professor working in KITS, Warangal, and Telangana. He has obtained Doctoral degree in the field of Alternative Fuels from Andhra University. He has more than 30 years of teaching experience and more than 20 International Journal Publications.